Journal of Engineering and Sustainable Development
http://jeasd.uomustansiriyah.edu.iq/index.php
https://doi.org/10.31272/jeasd.26.1.1

Vol. 26, No. 01, January 2022
ISSN 2520-0917

THE BEHAVIOR OF HEAT SINK-IMPINGEMENT COOLING WITH FLAT PLATE AND ARCED FINS MODELS

***Dalmn Y. Taha[1]** **Dhamyaa S. Khudhur[1]** **Layla M. Nassir[1]**

1) Mechanical Engineering Department, College of Engineering, Mustansiriyah University, Baghdad, Iraq

Received 8/3/2021 ***Accepted in revised form 12/6/2021*** ***Published 1/1/2022***

Abstract: In this paper, a statistical analysis was applied to the numerical predictions of temperature distribution for the heat sinks. There are two types of heat sink with an array of impingement. The first type is a flat plate heat sink, and the second type is arcs-fins heat sinks. The second type category considers five models (A, B, C, D, and E). The shapes of fins were changed, but the thickness, distance between fins, and radius were held fixed for comparing and analyzing them depending upon the improvement of the fin geometry of heat sink. The heat sinks of the two types are subjected to multi impinging flow at different Reynolds numbers (7000-11000). Thermodynamic and hydraulic results were collected. The best model was calculated through a statistical analysis. The efficiency of an arcs-fin heat sink was superior to that of the flat plate heat sink. The findings of Model D were more appropriate than those of the other models. The concave arc near the heat sink's exit (model D) created better effect than the convex arc (model E), despite the fact that the (model D) shape fins being identical to (model E) shape fins (only rotated 180° at the same location). However, Descriptive Statistics manifested that in all situations, the mean temperature for (model D) is better than (model E). The results of comparison between the flat plate heat sink and models (D and E) evinced that the average heat sink temperature in the suggested design reduced via 12%, 8%, while the (model E) decreased by 12%, 7% for Re (7000, 9000), respectively. In addition, the two models maintained the same percentage of (8% and 7%) improvement at Re (11000). The correlation coefficient between the flat plate and the arcs-fins heat sink for model B has the highest value (0.809), while model A has the lowest value of correlation (0.673).

Keywords: *Statistical analysis; Arcs-fin heat sink; Air; Array of impingement*

1. Introduction

The increasing of the flow rate, the surface area of heat sinks, or improving the flow distribution through the use of baffle barriers and other techniques, like parallel flow or impingement flow are the all ways that can help increase the electronic modules and packages cooling. All of these strategies have benefits, but they come at a cost. Raising the rate of flow is easy to do, but it necessitates greater and more efficient (air)-moving equipment, which increases the acoustic noise in addition to the total expense, weight, and volume of system. Due to the relatively high friction effects, this issue of enhancing the rate of heat transfer via raising the rate of flow is specially leading to cooling. This has a much smaller impact in liquids, where an improvement in the rate of flow causes a perfect heat transfer at a low expense in friction. The coefficient of heat transfer per unit area is obtained to differ as the ratio of velocity (v) to

**Corresponding Author*: ehma024@uomustansiriyah.edu.iq

the power (P) is around (0.7). The viscous influences, otherwise, are a function of (v) to (P) of (2 to 3), a much stronger function [1].

Generally, increasing the surface area, while lowering the velocity (v), is more efficient [2]. CPU cooling, audio amplifier cooling and power LED cooling are examples of passive cooling. In contrast to electronic devices, however, the method of passive heat sink hasn't advanced significantly. Most of the traditionally obtainable passive heat sinks being yet bulky and made of a sole material, like graphite or metal or. Only a few extrusion designs of fin have been investigated, and there has rarely been a requirement for further effectual module designs since the modules have historically been comparatively big. Savithri Subramanyam and Keith E. Crowe [3] identified how to use thermal finite element analysis (FEA) and (CFD) to test the designs of the electronic cooling heat sinks. Sathe and Sammakia studied a unique high-performance impingement heat sink. [1]. S. Zu and Yan [4] looked at how well seven turbulent models predicted the thermal and flow characteristics of a confined impinging jet. S. Manivannan S. et al. [5] proposed a Taguchi design of experiments-based Grey relational analysis method for multi-objective optimization of the flat plate heat sink. ANOVA test was used to determine the contribution and effect of each heat sink design factor on the heat sink's multiple responses. Mathias Ekpu et al. [6] improved the thermal management and microelectronics package efficiency. M. Beriache et al. 2012 [7] investigated the numerical simulation of the plate-fin heat sinks with confined impingement cooling. Simple model was developed to predict the thermal and hydraulic efficacies of the plate fin heat sink for impingement air cooling. Finite difference method (FDM) was utilized for converting the governing equations to algebraic formulas. Multiple grid sizes were used, then a (42 × 37 × 66) grid was chosen to show that the solution became nearly independent of the size of grid, as well as more increment in the grids wouldn't possess an important influence upon the solution. Also, the outcomes of this preparation were satisfactory leading to infer that the computational correctness of the field parameters was independent of the nodes' number while having (102,564) or further. The effect of base thickness and fin height upon the thermal efficacy of heat sinks made from aluminum and copper being investigated using a steady-state thermal conduction analysis. Lemos and Dorea provided numerical results for a a turbulent jet impinging on a flat plane covered with a sheet of permeable and thermally conducting material. [8]. Yang et al. [9] studied the turbulent fluid flow and the heat transfer characteristics of the air jet impingement onto rotating and stationary heat sinks using numerical simulations. The effects of impingement cross-flows on reducing the local surface Nusselt numbers as the impingement jets were deflected and became less coherent were shown by Junsik Lee et al [10]. K. Marzec and A. Kucaba-Pietal, 2014 [11] used an array of (6) impingement jets. Chamfer and countersunk nozzle type were used to study the numerical analysis of a flow characteristic, the coefficient of heat transfer (h), (Nu) distribution and pressure drop (ΔP). Results manifested that using an array of cooling jets gave a uniform (ΔP) distribution. Also, the biggest deflection angle was observed in the chamfer nozzle configuration. Where, the lowest (ΔP) takes place through the analysis with the nozzles countersunk kind. The presented analysis showed that (h) relies upon the flow direction whilst air entering the nozzle. Roaad K. Mohammed A. [12] examined experimentally the local distribution of heat transfer coefficients

between the impinging jets from a circular orifice on a flat plate. Jet-to-plate spacing was varied from (2 to 8) orifice diameters, and (Re) was varied between (7100 and 44400). P. Chandramohan et al. [13] investigated the temperature, Nusselt number, and heat transfer coefficient of a hot plate that were exposed to multi-jet air impingement cooling in an experimental environment and by using ANOVA analysis found that the important participations upon the responses were owing to the ratio of (H/D) ratio as well as the Re no. influence.

Xiaoming Huang et al. [14] examined three various dimple designs: convex, concave and mixed). The exterior faces alongside the model channel were presumed to be adiabatic and considered the geometric and boundary symmetry of the micro channel heat sink with impinging jets (MIJ) with dimples alongside the X and Y axes and simulated its model. The (MIJ) having dimples being compared with the MIJ having no dimples. Result showed that the use of convex dimples to (MIJs) improved the flow of fluid and the heat transfer, comparative to the other kinds. Gao Apeng et al. [15] used a computational simulation to analyze the features of impingement cooling before evaluating and improving the structure. Archibald Allswell Amoako [16] developed a numerical technique to test thirteen various heat sink geometries employing CFD program, as well as simple and exotic heat sink fin designs which improved the thermal efficiency of heat sink. Hassan Khurshid et al. [17] identified an empirical approach to the design and construction of a passive heat sink for an ABB communication board that was used in it. Based on the natural convection, two traditional fin geometries, rectangular plate fins, and rectangular pins fins were considered. Patrick McInturff et al. 2018 [18] improved the efficiency and the rise levels of the surface heat transfer of impingement cooling by adding special patterns of surface roughness to the impingement target surfaces. Circle, racetrack, and triangle were the (3) various impingement hole **configuration**s that utilized inside a jet array. Each of the three hole shapes had the similar hydraulic diameter. Data were presented at (Re = 900, 1500, 5000, and 11,000). Result depicted that the shape of racetrack hole gives the similar rise of heat transfer as a circle hole shape, with somewhat better efficiency, at certain circumstances. Differently, the triangle hole shape gives lower rising in the heat transfer, comparably with the racetrack hole and circle hole shapes. The swirl jet impingement effect was studied experimentally and numerically by N. V. S. Shankar and H. Ravi Shankar [19], by using swirl generators, it was possible to raise the turbulence of the impinging plane. On a flat plate, 33 swirl jets were impinged. **Ammar A.** Hussain et al. [20] searched and improved the convective heat transfer of the plate-fin heat sinks. Two geometries were investigated: plate-fin heat sinks without fillet profile and plate-fin heat sinks with fillet profile. Impinging (traditional design) and parallel flow were added to the investigation. The computational grid was developed using ANSYS Fluent for discretizing and solving the governing equations. **Mohamed** L. Elsayed et al. [21] investigated the efficiency of a partial shield heat sink for various open area ratios, as well as the effect of inserting the guide plate at various inclination angles. Paweł Gil and Joanna Wilk, [22] used a synthetic jet to investigate the heat transfer phenomenon that occurs during the impingement cooling.

In this article, ANOVA was used in two ways, based on the numerical results of using ANSYS Fluent (2019-R1). The aims of the study are to determine the best heat sink configuration and the connection between the flat plate and the

arcs-fin heat sinks using a new fin-heat sink arrangement with different geometries. The use of an impingement jet in combination with a heat sink can also assist in the dissipation of heat from an electronic device. Finally, the thermal and flow fields of a modern heat sink as a result of new multi jet impingement characteristics will be analyzed. According to a review of the literature, there has not been a statistical analysis work on a multi-jet impingement over the finned-heat sink arrays in arcs shapes. Arcs were designed in a range of ways, including fins with the same number of fins arrayed, and exposure to air from jets arrayed. The first model has the same form of concave arcs at a constant radius. This model has changed to have two concave arcs and two convex arcs in different locations at the same radius. The focus of the study is on the effect of arcs types and the location of it on heat dissipation by new impingement jet array. To get an enhancement for electronic cooling, one needs the best alternative model for the flat plate heat sink. A suitably modified version of the three-dimensional impingement jets over the arcs-fins heat sink has been used. Computational fluid dynamic model is created depending on the test description and by the software package Fluent examined using ANSYS Fluent (2019-R1). Then, the numerical results were used in a statistical analysis in two-way (ANOVA).

2. Physical Model

The forced convection and conduction heat transfer from a 60 mm× 60 mm discrete heat source (8333.33 w/m^2) using an arcs-fin heat sink were investigated. The heated part was flush mounted on the enclosure base, and the arcs-fin array was connected to it. The heat sink was cooled using a multi jet impingement. The parameters of jet impingement and heat sink used in this study are shown in Table (1) and Table (2). While, Table (3) views the comparison of the arcs-fins heat sink geometry specifications, and figure (1) manifests the design models of the present study.

Table 1. Description modeled of the multi air jet

(n-1 x n-5)	6×2
No. of jets	12
Diameter of nozzle	5 mm
Span wise of jet array	8 mm
Stream wise of jet array	28 mm
Jet to target plate spacing	30 mm
Jet Reynolds based on jet velocity	7000-9000-11000

Table 2. Description modeled of heat sink

Length	60 mm
width	60 mm
Height of base	6 mm
Number of fins	14
Fin thickness	3 mm
Number of fins row	2
Space between two row	5 mm
Height of fin	20 mm
S_T	28 mm
S_L	8 mm
Length of fin	20 mm
Radius of arc fin	45 mm

Table 3. Comparison of the arcs- fins Heat sink Geometry Specifications

Model	No. of concave arc	Shapes configuration
A	*4*	Symmetric concave arcs
B	*2*	Symmetric concave–convex arcs
C	*2*	Series concave arcs in z direction of fin
D	*2*	Series concave arcs in the fin x direction (divergent from the heat sink middle)
E	*2*	Series concave arcs in the fin x direction (convergent from the heat sink middle)

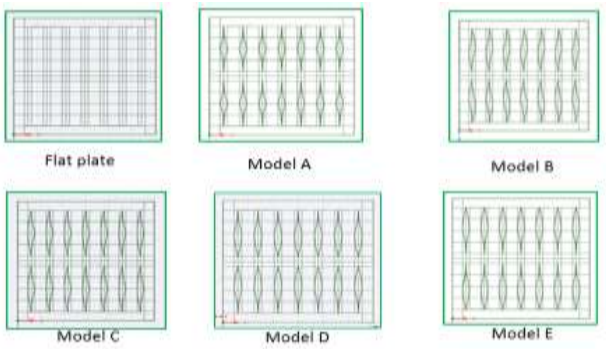

Figure 1. The tested design of the present study

3. Meshing of the Domain

The domain of computation and modeling used (7 × 2) arcs-fin heat sink with (6 × 2) nozzle array. The number of different meshes was tested at Re (7000, 9000, and 11000) for five cases of fins heat sink added to the flat plate heat sink. The assembly meshing was added to that, and Table (4) views its numbers. While, figure (2) reveals the computational mesh for the geometry of enclosure with different heat sink configurations:

Flat plate, models (A- B- C- D- E).

Table 4. The effect of the amount of grid element on the collected data

The shape	Nodes	Elements
Base Heat Sink	379458	2123624
Model A	1017046	5356320
Model B	748666	3948279
Model C	847713	4449055
Model D	983274	5165997
Model E	769701	4038323
Assembly Meshing	726316	3814457

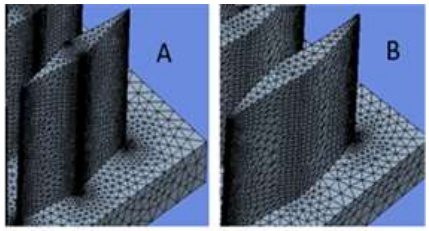

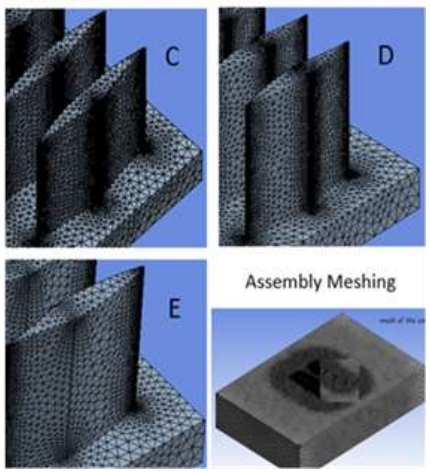

Figure 2. Meshing of the arcs-fin heat sink and computation domain

4. Conservation Equations and Boundary Conditions

Conservation of continuity equation is:

$$\frac{\partial(u)}{\partial x}+\frac{\partial(v)}{\partial y}+\frac{\partial(w)}{\partial z}=0 \qquad (1)\ [23]$$

Conservation of the linear momentum equation for steady state:

– x- Component

$$u\frac{\partial(u)}{\partial x}+v\frac{\partial(u)}{\partial y}+w\frac{\partial(u)}{\partial z}=-\frac{1}{\rho}\frac{\partial P}{\partial x}+\frac{\partial}{\partial x}\Big[(\mu+\mu_t)\left(2\frac{\partial u}{\partial x}\right)\Big]+\frac{\partial}{\partial y}\Big[(\mu+\mu_t)\left(\frac{\partial u}{\partial y}+\frac{\partial v}{\partial x}\right)\Big]+\frac{\partial}{\partial z}\Big[(\mu+\mu_t)\left(\frac{\partial u}{\partial z}+\frac{\partial w}{\partial x}\right)\Big] \qquad (2)$$

- y - Component

$$u\frac{\partial(v)}{\partial x}+v\frac{\partial(v)}{\partial y}+w\frac{\partial(v)}{\partial z}=-\frac{1}{\rho}\frac{\partial P}{\partial y}+\frac{\partial}{\partial x}\Big[(\mu+\mu_t)\left(\frac{\partial v}{\partial x}+\frac{\partial u}{\partial y}\right)\Big]+\frac{\partial}{\partial y}\Big[(\mu+\mu_t)\left(2\frac{\partial v}{\partial y}\right)\Big]+\frac{\partial}{\partial z}\Big[(\mu+\mu_t)\left(\frac{\partial v}{\partial z}+\frac{\partial w}{\partial y}\right)\Big] \qquad (3)$$

z- Component

$$u\frac{\partial(w)}{\partial x}+v\frac{\partial(w)}{\partial y}+w\frac{\partial(w)}{\partial z}=-\frac{1}{\rho}\frac{\partial P}{\partial z}+\frac{\partial}{\partial x}\Big[(\mu+\mu_t)\left(\frac{\partial w}{\partial x}+\frac{\partial u}{\partial z}\right)\Big]+\frac{\partial}{\partial y}\Big[(\mu+\mu_t)\left(\frac{\partial w}{\partial y}+\frac{\partial v}{\partial z}\right)\Big]+\frac{\partial}{\partial z}\Big[(\mu+\mu_t)\left(2\frac{\partial w}{\partial z}\right)\Big] \qquad (4)$$

Energy equation

$$u\frac{\partial(T)}{\partial x}+v\frac{\partial(T)}{\partial y}+w\frac{\partial(T)}{\partial z}=\frac{\partial}{\partial x}\left[\left(\frac{\mu}{Pr}+\frac{\mu_t}{Pr_t}\right)\frac{\partial T}{\partial x}\right]+$$

$$\frac{\partial}{\partial y}\left[\left(\frac{\mu}{Pr}+\frac{\mu_t}{Pr_t}\right)\frac{\partial T}{\partial y}\right]+\frac{\partial}{\partial z}\left[\left(\frac{\mu}{Pr}+\frac{\mu_t}{Pr_t}\right)\frac{\partial T}{\partial z}\right] \quad (5)$$

For standard k-εmodel

K- equation

$$u\frac{\partial(k)}{\partial x}+v\frac{\partial(k)}{\partial y}+w\frac{\partial(k)}{\partial z}=\frac{\partial}{\partial x}\left[\left(\mu+\frac{\mu_t}{\sigma k}\right)\frac{\partial k}{\partial x}\right]+$$

$$\frac{\partial}{\partial y}\left[\left(\mu+\frac{\mu_t}{\sigma k}\right)\frac{\partial k}{\partial y}\right]+\frac{\partial}{\partial z}\left[\left(\mu+\frac{\mu_t}{\sigma k}\right)\frac{\partial k}{\partial z}\right]+P_k-\varepsilon \quad (6)$$

$\varepsilon-$ equation

$$u\frac{\partial(\varepsilon)}{\partial x}+v\frac{\partial(\varepsilon)}{\partial y}+w\frac{\partial(\varepsilon)}{\partial z}=\frac{\partial}{\partial x}\left[\left(\mu+\frac{\mu_t}{\sigma\varepsilon}\right)\frac{\partial\varepsilon}{\partial x}\right]+$$

$$\frac{\partial}{\partial y}\left[\left(\mu+\frac{\mu_t}{\sigma\varepsilon}\right)\frac{\partial\varepsilon}{\partial y}\right]+\frac{\partial}{\partial z}\left[\left(\mu+\frac{\mu_t}{\sigma\varepsilon}\right)\frac{\partial\varepsilon}{\partial z}\right]+[C_1f_1-$$

$$\rho C_2f_2\varepsilon]\frac{\varepsilon}{k} \quad (7)$$

Where:

$$P_k=\mu_t\left\{2\left[\left(\frac{\partial u}{\partial x}\right)^2+\left(\frac{\partial v}{\partial y}\right)^2+\left(\frac{\partial w}{\partial z}\right)^2\right]+\right.$$

$$\left.\left(\frac{\partial u}{\partial y}+\frac{\partial v}{\partial x}\right)^2+\left(\frac{\partial u}{\partial z}+\frac{\partial w}{\partial x}\right)^2+\left(\frac{\partial v}{\partial z}+\frac{\partial w}{\partial y}\right)^2\right\} \quad (8)$$

$P_{rt}=Turbulent\ Prandtl\ number$

$C_{1\varepsilon}=1.44, C_{2\varepsilon}=1.92,$

$\sigma_k=1.0, \sigma_\varepsilon=1.3,$

$f_1=f_2=1\ (for\ standard\ k-\varepsilon\ models)$

The computational domain is bounded by solid (heat sink) and fluid (air). The solution domain is filled with stagnant air. By supposing that the heat being produced in the heat sink at an even rate and can be denoted via (q°=c) from the bottom. To simplify the proposed model solution, the following assumptions are used:

- The working fluid is air, which has constant properties.
- The conditions are steady state.
- The heat sink's sides are insulated, only the fin surfaces and top surface of heat sink are exposed to convection.
- The comparative pressure being zero Pa, and the working temperature is 300 K, with (5%) turbulence.
- The air temperature is at (300 K).
- The model case is turbulence, and the standard k-ε model is used.
- The wall surface was in no-slip condition.
- Thermal conductivity is constant with the exception of variations in air density in the momentum equation's buoyancy term.
- There is no gravitational effect during impingement.
- The term of viscous dissipation is negligible.
- The heat sink is made of aluminum, which has a density of 2702 kg/m^3, a specific heat capacity of 903 J/kg. K, and (K) thermal conductivity (237 W/m.°C).
- The value of constant heat flux (8333.33W/m^2).

5. Analysis of Data Using SPSS Software

Analysis of variance (ANOVA analysis in the SPSS software) is a statistical models group and it is related estimation proceedings (like the "variation" between groups) utilized for analyzing the variation between group means in specimen. ANOVA has been developed by the statistician Ronald Fisher. It has been based on the total variance law, in which the observed difference in a special changeable is divided into components attributable to various variation sources. In its simplest shape, ANOVA provides a statistical test of whether two or more population means have been equal, so it generalizes the T-test beyond the two means. The temperature results obtained from these tests may utilize to study the difference between specimen and the significant influence of treatment and factors [24].

(SPSS) has been used for these considerations using two ways ANOVA, and Table (5) shows the summary of two ways ANOVA. [25].

While, figure (3) evinces the legends of numerical study that used in analysis.

Table 5. Two-way ANOVA summary

	DF	*SS*	*MS*	*F*	*F -critical*
Main effect A	A-1	A Variance $^{2 \times N}$	SSA / DFA	MSA / MSr	DFA, DFr
Main effect B	B-1	B Variance $^{2 \times N}$	SSB / DFB	MSB / MSr	DFB, DFr
Residual (Error)	Total –(A+B)	SS_{total} – (SSA + SSB)	SSr / DFr	N/A	N/A
Total	N-1	Standard deviation $^{2 \times (N-1)}$	N/A	N/A	N/A

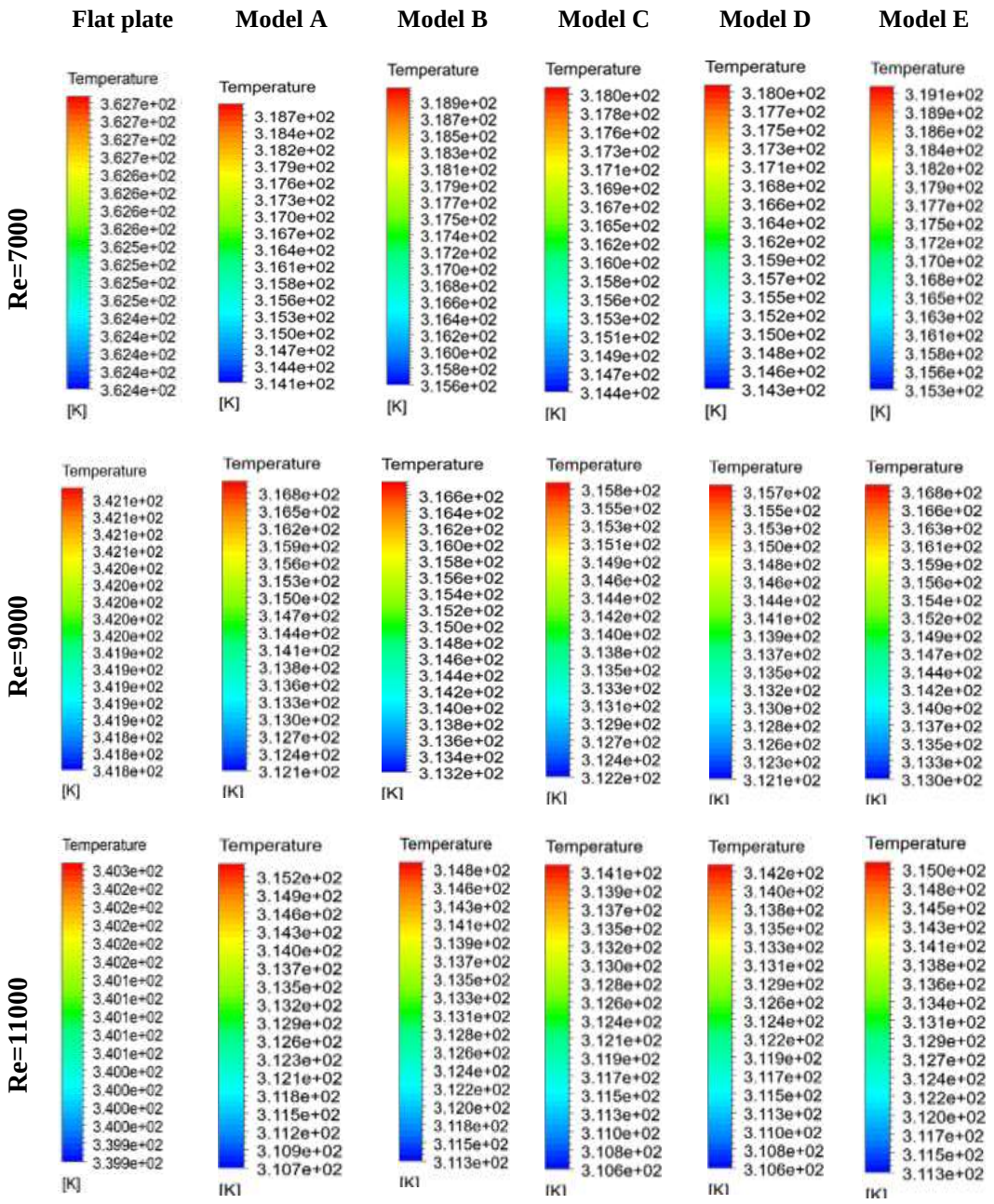

Figure 3. The legends of the numerical study input in analysis

5.1 SPSS Program for Data Analysis

SPSS is a statistical software package used for statistical analysis. The data for the numerical distribution temperatures were analyzed with SPSS program, those data were collected from a numerical work for temperature distribution with the variation of the effect of Reynolds number with a two-way variation analysis. The level of significance adopted during the analysis of the empirical results data for the research is a 95%. So, the accepted error ratio is 0.05. To test the effectiveness of factors, the calculated significance was compared with 0.05. If the calculated value is lower than (0.05), this means rejecting the hypothesis of non-absence and accepting the alternative hypothesis, which indicates that the variables are effective in the model. The opposite state (if the calculated value is greater than the value (0.05), which means that the variables are not affecting in the model [24].

5.2. ANOVA Tables Resulting From Data Analysis

The legend of the solid that resulted by using ANSYS Fluent (2019-R1) at Re (7000-9000-11000) for the two types of heat sink, were presented in (figure 1). Temperature distribution values represent the data entered in the statistical analysis. Table (6) displays the homogeneity of the values for Std. deviation, the closer values of the Std. deviation is to zero, the better it is. Table (7) shows that the value of (F- value for Reynolds number) is 226.162, while the value of (F-value for the model) is 7.413. This indicates that the Reynolds number index is better than the (model), considering Re. no. having the higher value. The table also elucidates that the Re. no intersection with the model is not significance at value (0.985). Because the significance value is more than 0.05.

Table 6. Descriptive Statistics

Dependent Variable: the temperature				
Re no	Model	Mean	Std. Deviation	*N*
1	A(1)	316.42353	1.455820	17
	B(2)	317.25556	1.023961	18
	C(3)	316.22941	1.127921	17
	D(4)	316.15294	1.148977	17
	E(5)	317.22941	1.187310	17
	Total	316.66512	1.265540	86
2	A(1)	314.43529	1.474339	17
	B(2)	314.90000	1.067708	18
	C(3)	313.98235	1.119283	17
	D(4)	313.91176	1.139014	17
	E(5)	314.91765	1.195949	17
	Total	314.43488	1.254804	86
3	A(1)	312.90588	1.423671	17
	B(2)	313.05294	1.092084	17
	C(3)	312.35882	1.113024	17
	D(4)	312.40000	1.148913	17
	E(5)	313.13529	1.177360	17
	Total	312.77059	1.213890	85
Total	A(1)	314.58824	2.034173	51
	B(2)	315.10755	2.018553	53
	C(3)	314.19020	1.942499	51
	D(4)	314.15490	1.919512	51
	E(5)	315.09412	2.053720	51
	Total	314.63074	2.022420	257

6. Results

In figure (4), the profile plot between the estimated marginal of the temperature and Re clarifies the effect of the arcs fins heat sink to dissipate the heat comparative with the flat plate heat sink. While in figure (5), the profile plot between the estimated marginal of the temperature and Re gives the models sort from the best to the worst (D, C, A, B, and E) (4, 3, 1, 2, and 5). Although the models (B, C, D, and E) are concave-convex arcs, but the model A is a concave arc, the models of the concave-convex arcs split into two groups: one group that provided better heat dissipation than model A. As for the second group, it performed below the A model and represented by the models B and E.

Table 7. Tests of Between-Subjects Effects.

Dependent Variable: the temperature

Source	Type III Sum of Squares	df	Mean Square	F	Sig.	Partial Eta Squared
Corrected Model	698.842a	14	49.917	34.688	.000	.667
Intercept	25429634.6	1	25429634.6	17671353.79	.000	1.000
Re	650.909	2	325.454	226.162	.000	.651
Model	42.668	4	10.667	7.413	.000	.109
Re * Model	2.678	8	.335	.233	.985	.008
Error	348.246	242	1.439			
Total	25442120.13	257				
Corrected Total	1047.087	256				

a. R Squared = .667 (Adjusted R Squared = .648)

The explanation for this case is the location of the concave arc, which generates large eddies. They are in viscid and interaction with flow, hence extracting energy from it. That leads to increase the rotation of large eddies and produce small eddies. The presence of a concave tail towards the edges of the heat sink is better.

The cooling improvement of the electronic modules and packages can be completed via a diversity of methods, like raising the flow rate of air, improving the air flow distribution, but maximizing the surface area of heat sinks may be increased or not if and only if the air flow distribution was improved. The numerical results of comparison between flat plate heat sink and the model D demonstrated that the average heat sink temperature in the suggested design reduces via 12% and 8% for Re (7000 and 9000), respectively. After the best model was determined, the five models were correlated with the flat plate heat sink. The results illustrated that there is a difference between the new model that will be manufactured and the basic one (flat plate). The relationship is not strong as the correlation value is closer to its value 1, the better it can be.

In other words, reaching a value of 1 means that the new model matches the basic model $0 \leq$ correlation ≤ 1. This state did not show through the results any mismatch, see figure (6).

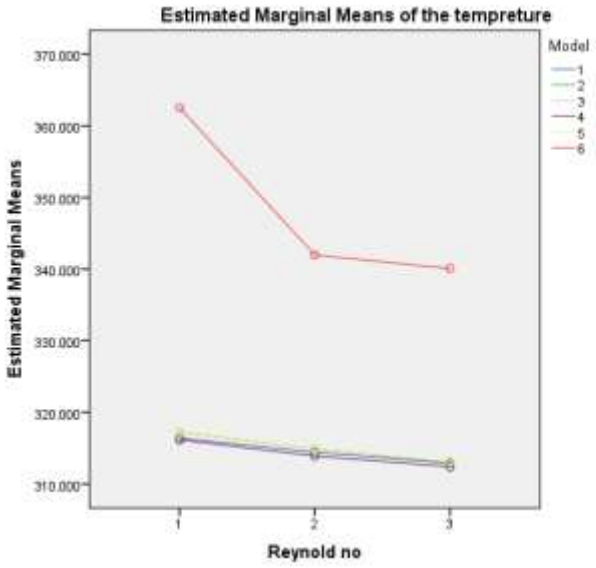

Figure 4. Profile plot between the estimated marginal of temperature and
Re (7000, 9000, and 11000) for flat plate with five models of AFHS

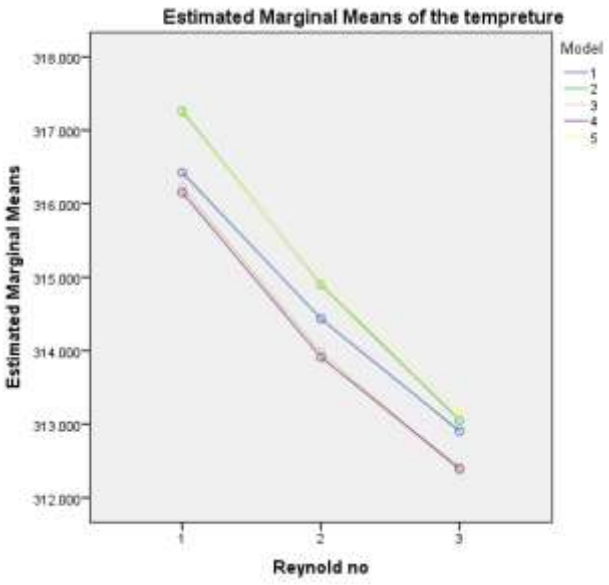

Figure 5. Profile plot between the estimated marginal of temperature and
Re (7000, 9000, and 11000) for (A-B-C-D-E) models

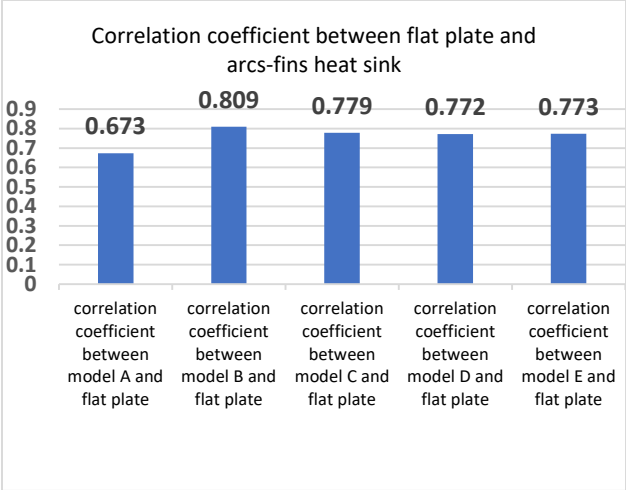

Figure 6. Values of the correlation coefficient between flat plate and arcs-fins heat sink

- The models (B, C, D and E) have the same numbers of concave-convex arcs and same volume. Added to that, model D is the same of the model E with only reflected, the result showed that the model E is the worst, while the model D is the best.
- Model A is better than model B, and model E instead of it has a smaller surface area than model (B-E).
- All state fin-heat sinks are in safety for uses and are better than the flat plate heat sinks.
- Model C is nearer to model D than the other models.
- Model B is nearer to model E than the other models.
- Improvement of the electronic modules and packages cooling can be talented if the air flow distribution was improved.
- Having a concave arc near the exit of heat sink (model D) gives better effect than having a convex arc (model E).

6.1 Validation

A validation case was recognized based on the research published in 2020 belongs to Basim Freegah, carried out for confirming that the outcomes got from the run of simulation being true, and the suppositions and the employed models being usable. By utilizing the numerical outcomes from Basim Freegah et al. [26] work on numerical analysis by using Plate-fin of Heat Sinks (PFHS) without fillet profile using the type of parallel flow. Across the z-axis, the coolant moves inside the heat sink. This state was taken to establish and prove the accuracy of the result. Table (8) views the geometry that taken in the validation.

Table 8. The geometry that taken in the validation

No. of fins	Length of base
10	40 mm
Thickness of base	Thickness of fin
5mm	1 mm
Width of base	Flow rate
39.7mm	0.0092 kg/s
High of fins	Space between two fins
20mm	3.3 mm

This model was built to be numerically solved by using ANSYS Fluent program with the same operation conditions. The validation result of the (PFHS) temperature at the rate of mass flow

(m° = 0.0092 kg/s) that obeys to parallel flow shows a good correspondence between both models, as shown in figure (7). The temperature distribution of freegah is (from 345.3 to 351.6) K, while in the present study, it is (from 347.1 to 352.8) K.

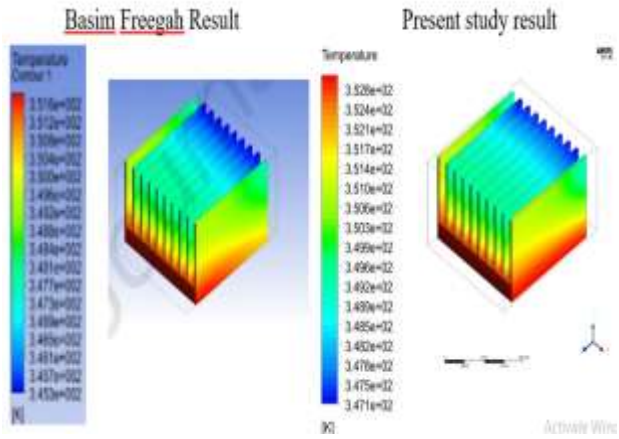

Figure 7. Comparison of the validation results of Freegah and present study

6.2 Comparison

A comparison with [26] of diverse designs in impinging flow for examining the thermal efficiency of the proposed designs if offered to impinging flow, and the base temperature at (m° = 0.0092 kg/s) have been presented for models (a-b-c-d-e-f).

Model (a) is a plate-fin heat sink without fillet profile, model (b) is a plate-fin heat sink with fillet profile, model (c) is symmetrical semicircle pins in a vertical arrangement, model (d) is corrugated semicircle pins in a vertical arrangement, and model (e) is symmetrical semicircle pins in a horizontal arrangement. Finally, model (f) is corrugated semicircle pins in a horizontal arrangement. All these models were compared with the base temperature counter for models (A-B-C-D-E) for the present study at Re (7000, 9000, and 11000) corresponding to the mass flow rate (0.00523 kg/s, 0.0067 Kg/s, and 0.008223 Kg/s), respectively. Anywhere, the temperature displays more active heat distribution. q° (18750 W/m^2), A (40 mm× 39.7 mm), and m° (0.0092 Kg/s) were used in (Basim Freege) study. The present study was presented in q° (8333.33 W/m^2), A (60 mm×60 mm). By changing the geometry and parameters of the fins-heat sink with changing the rate of mass flow, the improvement in the dispersion base cooling is achieved. All states of the arcs-fin heat sink have better result by comparing with the research view, see figure (8).

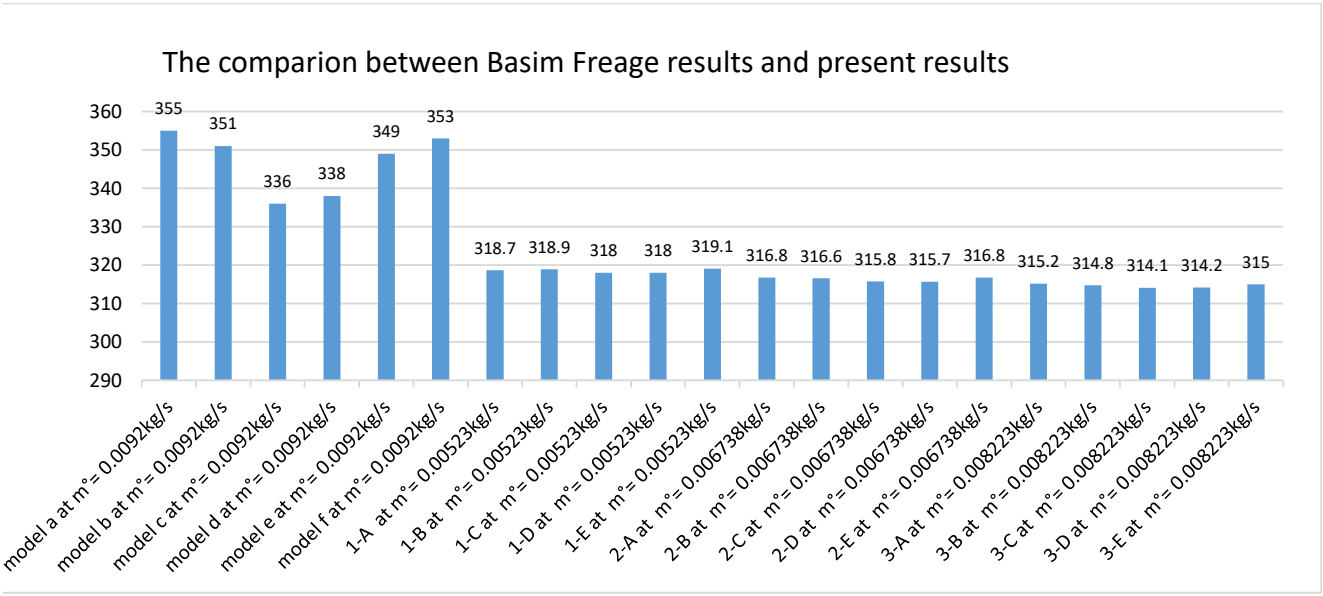

Figure 8. The comparative result between (Basim Freage) and

7. Conclusion

The increasing of Re for flat plate heat sink (conventional) enhances the dissipations of heat by 6% and 5% at Re (9000 and 11000), respectively. The new models of fins and the shapes that were chosen at the same thickness, distance between fins, length, height of fins, no. of fins, array of jets and its diameter were kept constant to be compared and analyzed depending on the geometry improvement of the heat sink fin. Under the same flow rate, the heat transfer performance of the arcs shape fin for model D appeared better among the other shapes of arcs fin (figure 4). However, the reflected shape (model E) leads to weaker performance. The results of comparison between flat plate heat sink and model (D, E) manifested that the average temperature of heat sink in the suggested design reduced via 12%, 8%, while the model E decreased by 12% and 7% for Re (7000 and 9000), respectively. The two models maintained the same percentage of (8% and 7%) improvement at Re (11000). The disadvantage with flow through the heat sinks is the rise in air temperature caused by upstream power dissipation. The heat sink design for a particular rate of flow and the air temperature inlet can finish up in a device, where the air comes in the heat sink at a slightly more temperature and can even bypass the heat sink. Careful study or testing is essential to the actual system condition; in order to confirm that the design is successful. Air impingement, in which the air being ducted straight to the heat sink as well as pushed into it, is one way to solve these challenges. Then, the flow rate and the air inlet temperature being further exactly understood. Such method being expensive since each implementation necessitates unique manifold, stiffener, heat sink, and the overall device of mechanical designs. Also, the impingement needs further space in the dimension vertical to the boards; to permit for the ducts and the manifolds directing the flow. But, the benefits are too important mainly for applications in great power by employing the air cooling.

Acknowledgment

The authors would like to thank Mustansiriyah University (http://www.uomustansiriyah.edu.iq), Baghdad-Iraq for the given support in accomplishing the present work.

Conflict of Interest

The authors confirm that the publication of this article causes no conflict of interest.

Abbreviations

l	Length of jet, mm
d	Diameter, mm
t_b	Thickness of plate, mm
q°	heat flux, $\frac{W}{m^2}$
H	height of fins ,mm
(n × n-5)	fin array
(n-1 × n-5)	hole array in Nozzle plate
R	Radius of each arc of fin, mm
S_L	longitudinal pitch of arc fin array, mm
S_T	transverse pitch of arc fin array, mm
Z/d	Ratio of the jet to the target plate spacing and nozzle
Re	Reynolds of the jet based upon the velocity of jet, $\frac{\rho_a u d_j}{\mu_a}$
A	Base area of heat sink, mm^2
Δp	Pressure drop, KPa
K	Thermal conductivity, $\frac{W}{m.c}$
DF	Degree of freedom
SS	Sum of squares
MS	Mean square
F	F values
F-critical	Critical statistics F
ANOVA	"Analysis of Variance"

8. References

1. S. B. Sathe B. G. Sammakia, *"An Analytical Study of the Optimized*

Performance of an Impingement Heat Sink", Transactions of the ASME, vol.126, pp. 528-534.

2. H. A. K. Shahad, T. A. Husain, and F. H. Ali, *"Experimental and Numerical Study of Fin Heat Sinks Systems"*, article in The Iraqi Journal for Mechanical and Materials Engineering, Nov. 2009, Des.20042.
3. Savithri subramanyam and Keith E. Crowe, 2000, *"Rapid design of heat sinks for electronic cooling computational and experimental tools"*, Sixteenth Annual IEEE Semiconductor Thermal Measurement and Management Symposium (Cat. No. 00CH37068), pp. 243-251, March 23-23, 2000, San Jose, CA, USA, 2000.
4. Y. Q. Zu Y. Y. Yan, *"Numerical Study on Stagnation Point Heat Transfer by Jet Impingement in a Confined Narrow Gap"*, Journal of Heat Transfer, vol. 131, No. 9, pp.1-4, 2009.
5. S. Manivannan, S. Prasanna Devi, R. Arumugam & N. M. Sudharsan,*"Multi-Objective Optimization of Flat Plate Heat Sink Using Taguchi-Based Grey Relational Analysis"*, Int J Adv Manuf Technol, vol. 52, 2010, pp. 739–749.
6. Mathias Ekpu, Raj Bhatti, Ndy Ekere, Sabuj Mallik, Emeka Amalu and Kenny Otiaba, *"Investigation of Effects of Heat Sinks on Thermal Performance of Microelectronic Package"*, 3rd IEEE Int. Conference on Adaptive Science and Technology, vol. 3, 2011, pp. 127- 132.
7. M. Beriache, A. Bettahar, H. Naji, L. Loukarfi and L. Mokhtar Saïdia, "Fluid Flow and Thermal Characteristics of a Minichannel Heat Sink with Impinging Air Flow", Arabian Journal for Science and Engineering, vol 37, no. 8, pp. 2243-2254, 2012.
8. Marcelo J. and S. de Lemos, *"Simulation of a Turbulent Impinging Jet into A Layer of Porous Material Using a Two–Energy Equation Model*", Numerical Heat Transfer, Part A, vol. 59, pp. 769-798, 2011.
9. Y.-T. Yang, S.-C. Lin, Y.-H. Wang, and J.-C. Hsu, *"Numerical Simulation and Optimization of Impingement Cooling for Rotating and Stationary Pin-Fin Heat Sink"*, International Journal of Heat and Fluid Flow, vol. 44, pp. 383-393. Des. 2013.
10. Junsik Lee, Zhong Ren, Phil Ligrani, Dae Hee Lee, Michael. Fox and Hee-Koo Moon, *"Cross-flow effects on impingement array heat transfer with varying jet-to-target plate distance and hole spacing International Journal of Heat and Mass Transfer"*, vol. 75, pp. 534 – 544 ,Aug. 2014.
11. K. Marzec and A. Kucaba-Pietal, "Heat transfer characteristic of an impingement cooling system with different nozzle geometry", Journal of Physics: Conference Series 530 -012038, pp.1-8, 2014.
12. Roaad K. Mohammed A., *"Air Impinging upon Target Plate Utilization Temperature Control under Variable Flow"*, M.Sc thesis, Mechanical Engineering Department, College of Engineering, Mustansiriayah University, 2014.
13. P. Chandra Mohan, S. N. Murugesan and S. Arivazhagan, *"Heat Transfer Analysis of Flat Plate Subjected to Multi Jet Air Impingement using Principal Component Analysis and Computational Technique"*, Journal of Applied Fluid Mechanics, vol. 10, no. 1, pp 293-306, 2016.
14. Xiaoming Huang, Wei Yang , Tingzhen Ming, Wenqing Shen and Xiangfei Yu, *"Heat transfer enhancement on a micro channel heat sink with impinging jets and dimples"***,** International Journal of Heat and Mass Transfer, vol 112, pp.113-124, 2017.
15. Gao Apeng, Lei Yubing and Jiang Yang *"Numerical Study of Impingement Cooling Under Constant Heat Flux"*, 2nd Int.

Conference on Automation, Mechanical Control and Computational Engineering (AMCCE 2017). Advances in Engineering Research, vol. 118 pp. 524 – 531.

16. Archibald Allswell Amoako, *"Optimization of Heat Sinks in a Range of Configurations"*, M.Sc Thesis, South Dakota State University, 2018.
17. Hassan Khurshid, Karthik Silaipillayarputhur and Tawfiq Al Mughanam, "Design of a Heat Sink for an Electronic Component in ABB Drive using Different Types of Fins", MATEC Web of Conferences 249, 03009, pp. 1-5, 2018.
18. Patrick McInturff, Masaaki Suzuki, Phil Ligrani, , Chiyuki Nakamata and Dae Hee Lee, "Effects of hole shape on impingement jet array heat transfer with small-scale, target surface triangle roughness", International Journal of Heat and Mass Transfer, vol. 127, pp. 585-597, 2018.
19. N. V. S. Shankar and H. Ravi Shankar, *"Experimental Investigation into Heat Transfer during Swirl Jet Impingement"*, International Journal of Applied Engineering Research, vol. 13, no. 7, pp. 4682-4687, 2018.
20. Ammar A. Hussain, Basim Freegah, Basima Salman Khalaf and Hossein Towsyfyan, *"Numerical investigation of heat transfer enhancement in plate-fin heat sinks: Effect of flow direction and fillet profile"*, Case Studies in Thermal Engineering, vol. 13, pp.1-14, 2019.
21. Mohamed L. Elsayed, Osama Mesalhy, Ramy H. Mohammed, John P. Kizito, Quinn H. Leland and Louis C. Chow, *"Enhancement of a heat sink performance using a partial shield and/or a guide plate"*, International Journal of Heat and Mass Transfer, vol. 134, pp. 948-958, May 2019.
22. Paweł Gil and Joanna Wilk, *"Heat transfer coefficients during the impingement cooling with the use of synthetic jet"*, International Journal of Thermal Sciences, vol. 147, no 2, pp. 1-9, Jan 2020.
23. G. Barakos, E.Mitsoulis and D. Assimacopoulos, "*Nutural Convection Flow in a Square Cavity Revisited: Laminar and Turbulent Models with Wall Functions*", International Journal for Numerical Methods in Fluids, vol. 18, pp. 695-719, 1994.
24. Raad Abd Al-Hassan Radhi,*"Investigation of creep properties for Hybridized Nano composites under Different Boundary Conditions with Statistical Analysis"*, M.Sc thesis, Mechanical Engineering Department, College of Engineering, Mustansiriayah University, 2020.
25. Aung Pyae,*" Quick calculation of Two-Way and One-Way ANOVA"*, (Experiment finding paper) Experiment Findings, June 2019, [online]. Available: https://www.researchgate.net/publication/333951232.
26. Basim Freegah, Ammar A. Hussain, Abeer H. Falih, and Hossein Towsyfyan, *"CFD analysis of heat transfer enhancement in plate-fin heat sinks with fillet profile: investigation of new designs"* Thermal Science and Engineering Progress, vol. 17, pp. 1-35, June 2020.